SUPPLEMENTAL MATERIAL

Here we address some technical aspects of the matrix product states (MPS) for non-Abelian quasiholes derived from conformal field theory (CFT) correlators. Similar to the treatment in the main text, we will leave the compactified U(1) boson implicit in the CFT description.

Fusion rules for the $\mathbb{Z}_3$ Read-Rezayi state

The $\mathbb{Z}_3$ Read-Rezayi state can be described by the $\mathbb{Z}_3$ parafermion conformal field theory [S1], also known as the minimal model $\mathcal{M}(5,6)$ [S2], with central charge $c = \frac{4}{5}$. The primary fields of this CFT are $(\mathbb{1}, \psi_1, \psi_2, \varepsilon, \sigma_1, \sigma_2)$, with scaling dimensions $(0, \frac{2}{3}, \frac{2}{3}, \frac{2}{5}, \frac{1}{15}, \frac{1}{15})$. The ψ_1 (resp. σ_1) field represents an electron (resp. a quasihole). The fusion rules of these fields are

	$\mathbb{1}$	ψ_1	ψ_2	ε	σ_1	σ_2
ψ_1	ψ_1	ψ_2	$\mathbb{1}$	σ_2	ε	σ_1
σ_1	σ_1	ε	σ_2	$\psi_2+\sigma_1$	$\psi_1+\sigma_2$	$\mathbb{1}+\varepsilon$

Fusion rules for the Gaffnian state

The Gaffnian wave function is described [S3] by the non-unitary CFT minimal model $\mathcal{M}(3,5)$, with central charge $c = -\frac{3}{5}$. The primary fields of this CFT are $(\mathbb{1}, \psi, \sigma, \varphi)$, with scaling dimensions $(0, \frac{3}{4}, -\frac{1}{20}, \frac{1}{5})$. The ψ (resp. σ) field represents an electron (resp. a quasihole), with fusion rules

	$\mathbb{1}$	ψ	σ	φ
ψ	ψ	$\mathbb{1}$	φ	σ
σ	σ	φ	$\mathbb{1}+\varphi$	$\psi+\sigma$

The MPS transfer matrix

Following the notation of Ref. [S4], we consider the transfer matrix $E = \sum_m^{0,1} (B^m)^* \otimes B^m$, where the B^m matrix is associated with an empty ($m=0$) or occupied ($m=1$) Landau orbital in the MPS. The transfer matrix is the basic building block of any generic wave function overlap $\langle\Psi|\Psi'\rangle$. It acts on a direct product of two copies of the truncated conformal Hilbert space, one copy for $\langle\Psi|$, and the other for $|\Psi'\rangle$. From the fusion rules, we find that the CFT Hilbert space can be naturally split into two sectors, each being closed under fusion with the electron (although they are connected by fusion with the quasihole). We refer to them as the "vac" and the "qh" sectors:

	vac	qh
Moore-Read	$\mathbb{1}, \psi$	σ
$\mathbb{Z}_3$ Read-Rezayi	$\mathbb{1}, \psi_1, \psi_2$	$\varepsilon, \sigma_1, \sigma_2$
Gaffnian	$\mathbb{1}, \psi$	σ, φ

The B^m matrices are block-diagonal in the sector index, $B^m = \bigoplus_\alpha B^m_\alpha$, with α summed over {vac, qh}. Therefore, the transfer matrix is also block-diagonal,

$$E = \bigoplus_{\alpha,\beta} E_{\alpha,\beta}, \text{ with } E_{\alpha,\beta} = \sum_m (B^m_\alpha)^* \otimes B^m_\beta. \tag{S1}$$

We denote by $\lambda^{(i)}_{\alpha,\beta}$ the i-th largest eigenvalue of $E_{\alpha,\beta}$. The MPS auxiliary space is constructed from the truncated conformal Hilbert space, and the truncation is constrained by the entanglement area law. In our calculations, we have to deal with transfer matrix blocks (after various reductions [S4]) with dimensions as large as

	(vac, vac)	(vac, qh)	(qh, qh)
Moore-Read	1.1×10^7	1.5×10^7	2.0×10^7
$\mathbb{Z}_3$ Read-Rezayi	3.6×10^7	5.5×10^7	8.4×10^7
Gaffnian	1.3×10^7	2.0×10^7	3.0×10^7

Incidentally, for the braiding and the overlap calculations, we have to work on the full direct product space without symmetry reduction, the dimension of which can be up to 25 times as large as the sizes mentioned in the previous table.

Overlap calculation

As explained in the main text, the central object in our braiding study is the overlap matrix $\langle abc|ab'c\rangle$, and we are particularly interested in its exponential convergence

$$\langle abc|ab'c\rangle = C_{abc}\delta_{bb'} + \mathcal{O}(e^{-|\Delta\eta|/\xi_{\langle abc|ab'c\rangle}}). \tag{S2}$$

In the following we outline the calculation of the overlap matrix using the MPS technique, and also discuss the determination of the correlation lengths. Recall from the main text that the state

$$|abc\rangle \equiv$$ 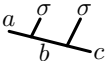

(S3)

involves two localized quasiholes at a finite separation $\Delta\eta$, and the topological charges a and c represent extra quasiholes pushed to the ends of the infinite cylinder. Diagrammatically, the MPS for $|abc\rangle$ is given by [S4, S5]

Here, the orbital B^m matrices are represented by the green circles, with the occupation number $m = 0, 1$ carried by the upward-pointing leg, and the quasihole matrices are represented by the purple squares. Each quasihole matrix depends on both the quasihole position and the fusion channel context, i.e. the topological charges before and after the σ field insertion in the fusion tree, and it is inserted into the matrix product at the correct time-ordered positions [S5]. Technical details of the construction of the quasihole matrix will be addressed in a forthcoming paper [S6]. The overlap $\langle abc|ab'c\rangle$ is computed by contracting

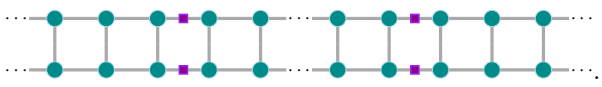

Here, the upper (lower) chain represents the $\langle abc|$ ($|ab'c\rangle$) state, respectively, and in the ladder-like structure, each rung corresponds to the transfer matrix E over a single orbital [Eq. (S1)]. Although not marked explicitly in the above diagrams, the fusion channel dependence enters through the quasihole insertions (purple squares) as well as the boundary conditions. The contraction of the above tensor network can be significantly simplified on an infinite cylinder, as detailed in Ref. S4. Essentially, an *infinitely* repeated action of the transfer matrix can be accurately represented by its projection into the subspace of its largest eigenvalue in the relevant sector. For the overlap $\langle abc|ab'c\rangle$ with a finite quasihole separation $\Delta\eta$, as shown in Fig. 4 of the main text, this simplification applies only to the peripheral regions outside of the two quasihole insertions. Between the two quasiholes, we have to contract the transfer matrices by brute force. However, in the limit of large $\Delta\eta$, asymptotically the overlap is still controlled by the leading few eigenmodes of the transfer matrix, and the associated correlation lengths can be simply determined from the spectral gaps of the transfer matrix, without resorting to curve fitting.

We now explain this using three representative examples. First, consider the off-diagonal element $\langle\sigma_1\psi_1\varepsilon|\sigma_1\sigma_2\varepsilon\rangle$ for the $\mathbb{Z}_3$ Read-Rezayi state. In this case, the action of the transfer matrix over the $\Delta\eta$ interval is confined to the (vac, qh) sector of the product space, while its action outside of the $\Delta\eta$ interval is purely in the (qh, qh) sector. At large $\Delta\eta$, we must have

$$\langle\sigma_1\psi_1\varepsilon|\sigma_1\sigma_2\varepsilon\rangle \sim \left(\frac{\lambda^{(1)}_{\text{vac,qh}}}{\lambda^{(1)}_{\text{qh,qh}}}\right)^{\Delta\eta/\gamma}. \tag{S4}$$

Here $\gamma = 2\pi\ell_0^2/L_y$ is the separation between adjacent Landau orbitals, while $\lambda^{(1)}_{\text{vac,qh}}$ and $\lambda^{(1)}_{\text{qh,qh}}$ are the largest eigenvalues of the transfer matrix in sectors (vac,qh) and (qh, qh), resp. The correlation length is then given by

$$\xi_{\text{ortho}} = \left[\frac{L_y}{2\pi\ell_0^2}\log\left(\frac{\lambda^{(1)}_{\text{qh,qh}}}{\lambda^{(1)}_{\text{vac,qh}}}\right)\right]^{-1}. \tag{S5}$$

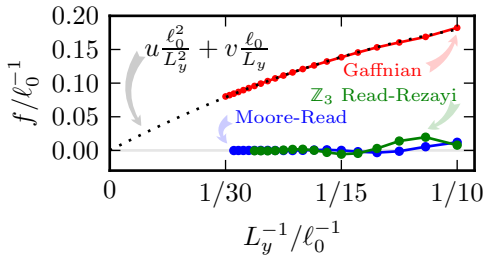

FIG. S1. Asymptotic repulsion f between two plasma charges representing pinned quasiholes. The Gaffnian curve is fitted by the zero-intercept quadratic formula $f\ell_0 = u\frac{\ell_0^2}{L_y^2} + v\frac{\ell_0}{L_y}$. The best fit has $u = -8.6(2)$ and $v = 2.66(1)$, with the standard error in the last digit given in parentheses.

As the second example, we consider the norm $\|\mathbb{1}\sigma\psi\|^2$ for the Moore-Read state. To the leading order, we have

$$\|\mathbb{1}\sigma\psi\|^2 \sim \left(\frac{\lambda^{(1)}_{\text{qh,qh}}}{\lambda^{(1)}_{\text{vac,vac}}}\right)^{\Delta\eta/\gamma}, \tag{S6}$$

while $\lambda^{(1)}_{\text{vac,vac}}$ and $\lambda^{(1)}_{\text{qh,qh}}$ are the largest eigenvalues of the transfer matrix in sectors (vac,vac) and (qh, qh), resp. For $\|\mathbb{1}\sigma\psi\|^2$ to approach a non-zero constant value when $\Delta\eta \to \infty$ as in Eq. (S2), we need to have $\lambda^{(1)}_{\text{vac,vac}} = \lambda^{(1)}_{\text{qh,qh}}$. This turns out to be true for the $\mathbb{Z}_{k=2,3}$ Read-Rezayi states, up to small finite-size corrections (see below). To characterize the exponential convergence of the norm, we have to consider the second largest eigenvalue in the (qh,qh) channel, $\lambda^{(2)}_{\text{qh,qh}}$. The associated correlation length is given by

$$\xi_{\text{qh}} = \left[\frac{L_y}{2\pi\ell_0^2}\log\left(\frac{\lambda^{(1)}_{\text{qh,qh}}}{\lambda^{(2)}_{\text{qh,qh}}}\right)\right]^{-1}. \tag{S7}$$

Finally, the correlation length associated with the norm $\|\sigma\psi\sigma\|^2$ for the Moore-Read state is similarly given by

$$\xi_{\text{vac}} = \left[\frac{L_y}{2\pi\ell_0^2}\log\left(\frac{\lambda^{(1)}_{\text{vac,vac}}}{\lambda^{(2)}_{\text{vac,vac}}}\right)\right]^{-1}. \tag{S8}$$

The numerical calculations of ξ_{vac} and ξ_{qh} are more challenging than ξ_{ortho}, since they depend on subleading eigenvalues of the transfer matrix. A detailed numerical study will be reported in a future paper [S7].

We now examine the $\lambda^{(1)}_{\text{vac,vac}} = \lambda^{(1)}_{\text{qh,qh}}$ condition more carefully. To have a physical understanding of its implication, we adopt the plasma analogy and reinterpret the

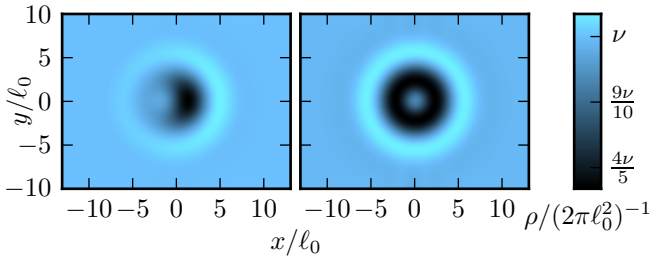

FIG. S2. Electron density around a single Gaffnian $\frac{e}{5}$ quasihole in the $|\mathbb{1}\sigma\rangle$ (left panel) and the $|\sigma\varphi\rangle$ (right panel) channels, on an infinitely long cylinder with perimeter $L_y = 20\ell_0$.

overlap in Eq. (S6) as the partition function $e^{-F(\Delta\eta)}$ with two pinned charges representing the two quasiholes at a separation $\Delta\eta$. The derivative of the free energy $F(\Delta\eta)$ with respect to $\Delta\eta$ gives an effective force between the plasma charges

$$f = -\frac{\mathrm{d}F}{\mathrm{d}\Delta\eta} \sim \frac{L_y}{2\pi\ell_0^2} \log\left(\frac{\lambda^{(1)}_{\mathrm{qh,qh}}}{\lambda^{(1)}_{\mathrm{vac,vac}}}\right). \tag{S9}$$

Therefore, if $\lambda^{(1)}_{\mathrm{vac,vac}} \neq \lambda^{(1)}_{\mathrm{qh,qh}}$, the two plasma charges representing quasiholes are subject to an asymptotically constant confining (if $f < 0$) or anti-confining (if $f > 0$) force that persists even in the limit of infinite separation. The numerical data are shown in Fig. S1. For the Moore-Read and the $\mathbb{Z}_3$ Read-Rezayi states, $\lambda^{(1)}_{\mathrm{vac,vac}}$ and $\lambda^{(1)}_{\mathrm{qh,qh}}$ quickly converge as L_y increases. In contrast, the Gaffnian state features an asymptotic repulsion between infinitely separated plasma charges at a finite cylinder perimeter L_y, although it seems to die off in the planar limit $L_y \to \infty$. This makes it very hard to extract a meaningful correlation length for the diagonal elements of the overlap matrix similar to Eq. (S7). Fortunately, we can still analyze the correlation length associated with the asymptotic orthogonality of conformal blocks, as discussed in the main text.

Electron density profile around Gaffnian quasiholes

Here we show more details of the peculiarities in the electron density profile of the Gaffnian quasiholes. As noted in the main text, conformal blocks in different fusion channels are locally distinguishable despite the clear separation between quasiholes. This effect persists even when we push the quasihole separations to infinity, leaving only a single fully isolated quasihole. In this limit, the conformal blocks can be labeled by fusion tree segments

$$|ab\rangle \equiv \begin{array}{l} a \quad \sigma \\ \diagdown\!\diagup \\ \quad b. \end{array} \tag{S10}$$

We only need to consider $|ab\rangle = |\mathbb{1}\sigma\rangle$ and $|\sigma\varphi\rangle$, since all the other possibilities can be obtained by either fusing (trivially) with ψ, or flipping the cylinder axis $x \to -x$. Fig. S2 shows the electron density profile for each case. The anisotropic dipole structure is clearly visible for $|\mathbb{1}\sigma\rangle$, in contrast to the isotropic $|\sigma\varphi\rangle$.

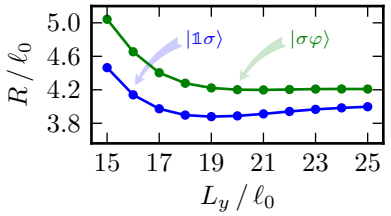

FIG. S3. Radii of Gaffnian quasiholes in $|\mathbb{1}\sigma\rangle$ and $|\sigma\varphi\rangle$ channels, as a function of the cylinder perimeter L_y.

Similar to the $\mathbb{Z}_{k\leq 3}$ Read-Rezayi quasiholes analyzed in the main text, we estimate the quasihole radius from the second moment of the charge excess distribution [Fig. S3]. We have also examined the Abelian charge $\frac{2e}{5}$ quasihole obtained by fusing two $\frac{e}{5}$ quasiholes in the $\mathbb{1}$ channel. We find a localized and isotropic density reduction around each Abelian quasihole, but this calculation turns out to be rather susceptible to the conformal Hilbert space truncation, and we have trouble reaching convergence in the radius calculation. As a final comment, we note that the peculiarities observed in the density profile are likely related to the leading eigenvalue mismatch discussed in the previous section, and are possibly artifacts at finite cylinder perimeter L_y. Unfortunately, we cannot resolve this issue using the current MPS approach, due to the fundamental constraint on L_y from the area law of quantum entanglement.

[S1] N. Read and E. Rezayi, Physical Review B **59**, 8084 (1999).

[S2] P. Di Francesco, P. Mathieu, and D. Sénéchal, *Conformal Field Theory* (Springer, 1999).

[S3] S. H. Simon, E. H. Rezayi, N. R. Cooper, and I. Berdnikov, Physical Review B **75**, 075317 (2007).

[S4] B. Estienne, N. Regnault, and B. A. Bernevig, ArXiv e-prints (2013), arXiv:1311.2936 [cond-mat.str-el].

[S5] M. P. Zaletel and R. S. K. Mong, Physical Review B **86**, 245305 (2012).

[S6] Y.-L. Wu, B. Estienne, N. Regnault, and B. A. Bernevig, (2014), in preparation.

[S7] B. Estienne, N. Regnault, and B. A. Bernevig, (2014), unpublished.